Relation between the kernel polynomial method and the bond-order potential

T. Qin*
School of Physical Sciences, University of Kent, Canterbury CT2 7NH, United Kingdom
(Received 1 October 2009; revised manuscript received 9 November 2009; published 16 February 2010)

The kernel polynomial method and the bond-order potential are two well-known linear scaling approaches in constructing interatomic potentials. They have been developed from different backgrounds in parallel, and the link between them has not been analyzed before. This Brief Report will demonstrate their close link by deriving the kernel polynomial method in the similar procedure that the analytic bond-order potential was constructed. An expression of bond order can also be derived from the kernel polynomial method; subsequently, the kernel polynomial method has a similar force expression as the analytic bond-order potential. Finally we will show that the kernel polynomial method, like the analytic bond-order potential, is also able to explain the structural trend across the nonmagnetic transition-metal series.

DOI: 10.1103/PhysRevB.81.073104 PACS number(s): 71.15.Nc, 71.20.Be

The tight-binding (TB) method[1–3] has been increasingly regarded as a promising approach to achieve accurate results at atomistic level. The TB method is much less computationally demanding than the *ab initio* method, however, the computational time of direct diagonalization of the Hamiltonian matrix remains an $O(N^3)$ problem. For large systems, it is necessary to calculate the bond energy with better scaling, ideally linear scaling. Among many $O(N)$ approaches,[4–15] the kernel polynomial method (KPM) (Refs. 4–6) has been established based on a mathematical expansion of the density of states through the first-kind Chebyshev polynomials, and the bond-order potential (BOP) (Refs. 9 and 16) was introduced based on a semi-infinite linear Lanczos chain. Recently the analytic BOP has been derived through the second-kind Chebyshev polynomials.[10]

The different behavior of the KPM and the BOP has been compared in literature,[6,17] however, the link between these two linear algorithms has not been analyzed before. In order to demonstrate their close relation, in this Brief Report the KPM will be derived in a similar procedure to the analytic BOP. The link between these two approaches and the Ducastelle and Cyrot-Lackmann theorem[18] will be analyzed, which will explain the well-known trend of the structural stability across the nonmagnetic transition-metal series.

Here only the relevant aspects of the TB method will be described.[19–21] The elements of the Hamiltonian matrix can be expressed as $H_{i\alpha,j\beta}=\langle i\alpha|\hat{H}|j\beta\rangle$, and the atom-centered orbitals $|i\alpha\rangle$ are assumed to be orthogonal, where i is the atom index and α denotes the five valence d orbitals. The diagonal elements of the Hamiltonian matrix are the on-site energies and are denoted as $E_{i\alpha}=H_{i\alpha,i\alpha}$. The bond energy then may be written as

$$U^{\text{bond}} = 2\sum_{i\alpha}\int^{E_F}(E-E_{i\alpha})n_{i\alpha}(E)dE, \tag{1}$$

where $n_{i\alpha}(E)$ is the local density of states and E_F is the Fermi-energy level.

Defining $n_i(E)$ as the average density of states for d-valent atom i

$$n_i(E) = \frac{1}{5}\sum_{\alpha=1}^{5} n_{i\alpha}(E), \tag{2}$$

then the bond energy associated with each individual site i can be expressed as

$$U_i^{\text{bond}} = 10\int^{E_F}(E-E_i)n_i(E)dE. \tag{3}$$

With $\hat{G}(Z)=(Z-\hat{H})^{-1}$, the matrix elements of the Green's function are $G_{i\alpha,j\beta}(Z)=\langle i\alpha|\hat{G}(Z)|j\beta\rangle$. The local density of states can then be expressed in terms of $G_{i\alpha,i\alpha}(Z)$ as[9]

$$n_{i\alpha}(E) = -\frac{1}{\pi}\lim_{\eta\to 0^+}\text{Im}\, G_{i\alpha,i\alpha}(E+i\eta). \tag{4}$$

Equation (4) is useful, since the Green's function can be written in terms of a continued fraction, whose components are related to moments as following.[22–24]

Starting from an initial orbital $|u_0\rangle$, the further orbitals can be generated through a recursion relation[7,22]

$$b_{n+1}|u_{n+1}\rangle = \hat{H}|u_n\rangle - a_n|u_n\rangle - b_n|u_{n-1}\rangle, \tag{5}$$

and we have

$$\langle u_m|\hat{H}|u_n\rangle = \begin{cases} a_n & \text{if } m=n \\ b_n & \text{if } m=n-1 \\ b_{n+1} & \text{if } m=n+1 \\ 0 & \text{otherwise} \end{cases} \tag{6}$$

with $n\geq 0$ and $b_0=0$. This recursion process can be illustrated through a semi-infinite linear chain shown in Fig. 1.

By setting $|u_0\rangle$ as the orbital $|i\alpha\rangle$, $G_{i\alpha,i\alpha}(Z)=\langle u_0|\hat{G}|u_0\rangle = \langle u_0|(Z-\hat{H})^{-1}|u_0\rangle$ can be written as a continued fraction[22]

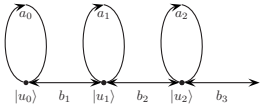

FIG. 1. The semi-infinite linear chain.

$$G_{i\alpha,i\alpha}(Z) = \cfrac{1}{Z - a_0 - \cfrac{b_1^2}{Z - a_1 - \cfrac{b_2^2}{Z - a_2 - \cfrac{b_3^2}{\ddots}}}}, \tag{7}$$

where the coefficients a_n and b_n can be expressed in terms of moments.[10] The nth moment of $|i\alpha\rangle$ is defined as

$$\mu_{i\alpha}^{(n)} = \int_{-\infty}^{\infty} E^n n_{i\alpha}(E) dE. \tag{8}$$

Using the above recursion method and a proper truncation scheme,[9] the local density of states is written as a function of moments by substituting Eq. (7) into Eq. (4). By substituting Eq. (4) into Eq. (1), the bond energy is calculated. This is the procedure to calculate the bond energy in the *numerical* BOP.[9]

A simple way to approximate $n_i(E)$ is to take constant recursion coefficients $a_n = a_{i\infty}$ and $b_n = b_{i\infty}$ for atom i. This results in a semielliptic density of states[7]

$$\tilde{n}_i(\epsilon) = \frac{2}{\pi}\sqrt{1-\epsilon^2}, \tag{9}$$

where ϵ is the band energy E normalized by $\epsilon = (E - a_{i\infty})/(2b_{i\infty})$, and $\tilde{n}_i(\epsilon) = \tilde{n}_i(E) \times 2b_{i\infty}$. An extension of $n_i(\epsilon)$ can be obtained by writing the average density of states as

$$n_i(\epsilon) = \tilde{n}_i(\epsilon) + \delta n_i(\epsilon). \tag{10}$$

Chebyshev polynomials of the second kind $P_m(\epsilon)$ are orthonormal with respect to the weight function $\frac{2}{\pi}\sqrt{1-\epsilon^2}$ which is just Eq. (9).[25] By taking advantage of these properties of $P_m(\epsilon)$, the formalism of the *analytic* BOP has been established.[10] The results will be summarized and compared with the KPM in Table I later.

The procedure to construct the analytic BOP can be seen in Ref. 10. Now we will derive the KPM in a similar manner to the analytic BOP. The *semi-infinite* linear chain in Fig. 1 can be extended to the left according to Eq. (5). As a result,

TABLE I. Formulas within the KPM and the BOP. "r" means to replace the value of $\hat{\chi}_m(\epsilon_F)$ and the associated Chebyshev parts, such as P_m for T_m and p_{mn} for t_{mn}.

	KPM	BOP
Chebyshev	First kind	Second kind
	$T_m(\epsilon) = \Sigma_{n=0}^m t_{mn}\epsilon^n$	$P_m(\epsilon) = \Sigma_{n=0}^m p_{mn}\epsilon^n$
$\tilde{n}_i(\epsilon)$	Eq. (12)	Eq. (9)
$\hat{\chi}_m(\epsilon_F)$	Eq. (24)	Eq. (25)
$\sigma_i^{(m)}$	Eq. (17)	r
$n_i^{n_{max}}(\epsilon)$	Eq. (20)	r
N_i	Eq. (27)	r
U_{bond}	Eq. (26)	r
$\tilde{\Theta}_{i\alpha j\beta}$	Eq. (29)	r
F_k^{bond}	Eq. (28)	r

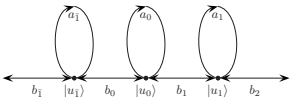

FIG. 2. The infinite linear chain.

now n can take negative integers and the condition of $b_0 = 0$ is removed. For simplicity $|u_{\bar{1}}\rangle$ will be used to denote $|u_{-1}\rangle$, similarly, $a_{\bar{1}}$ for a_{-1} and $b_{\bar{1}}$ for b_{-1}. Accordingly, this recursion can be described by an *infinite* linear chain shown in Fig. 2.

From this linear chain, a different $G_{i\alpha,i\alpha}(Z)$ can be obtained as

$$G_{i\alpha,i\alpha}(Z) = \cfrac{1}{Z - a_0 - \cfrac{b_1^2}{Z - a_1 - \cfrac{b_2^2}{Z - a_2 - \cfrac{b_3^2}{\ddots}}} - \cfrac{b_0^2}{Z - a_{\bar{1}} - \cfrac{b_{\bar{1}}^2}{Z - a_{\bar{2}} - \cfrac{b_{\bar{2}}^2}{\ddots}}}}. \tag{11}$$

If constant coefficients $a_n = a_{i\infty}$ and $b_n = b_{i\infty}$ are taken for Eq. (11), we can finally have

$$\tilde{n}_i(\epsilon) = \frac{1}{\pi\sqrt{1-\epsilon^2}}. \tag{12}$$

It is known that the Chebyshev polynomials of the first kind $T_m(\epsilon)$ are orthogonal with respect to Eq. (12):[25]

$$\int_{-1}^{1} \frac{1}{\pi\sqrt{1-\epsilon^2}} T_n(\epsilon) T_m(\epsilon) d\epsilon = \begin{cases} 0 & n \neq m \\ 1 & n = m = 0 \\ 1/2 & n = m \neq 0. \end{cases} \tag{13}$$

$T_m(\epsilon)$ satisfies the recurrence relation[25]

$$T_{m+1}(\epsilon) = 2\epsilon T_m(\epsilon) - T_{m-1}(\epsilon) \tag{14}$$

with $T_0(\epsilon) = 1$ and $T_1(\epsilon) = \epsilon$.

$T_m(\epsilon)$ can be expressed by their coefficients t_{mn}:[25]

$$T_m(\epsilon) = \sum_{n=0}^{m} t_{mn}\epsilon^n. \tag{15}$$

By expanding $\delta n_i(\epsilon)$ in Eq. (10) in terms of $T_m(\epsilon)$, $n_i(\epsilon)$ can be written as

$$n_i(\epsilon) = \frac{1}{\pi\sqrt{1-\epsilon^2}}\left[1 + \sum_{m=1} \sigma_i^{(m)} T_m(\epsilon)\right]. \tag{16}$$

By taking advantage of the orthogonal properties of $T_m(\epsilon)$ in Eq. (13), $\sigma_i^{(m)}$ can be expressed as

$$\sigma_i^{(m)} = \int_{-1}^{1} T_m(\epsilon) n_i(\epsilon) d\epsilon = \sum_{n=0}^{m} t_{mn} \hat{\mu}_i^{(n)} \quad \text{for} \quad m \geq 1, \tag{17}$$

where

$$\hat{\mu}_i^{(n)} = \int_{-1}^{1} n_i(\epsilon)\epsilon^n d\epsilon. \tag{18}$$

By substituting $\epsilon=(E-a_{i\infty})/(2b_{i\infty})$ into Eq. (18), we have

$$\hat{\mu}_i^{(n)} = \frac{1}{(2b_{i\infty})^n}\sum_{l=0}^{n}\binom{n}{l}(-1)^l a_{i\infty}^l \mu_i^{(n-l)}. \tag{19}$$

By substituting Eq. (17) into Eq. (16), eventually we have

$$n_i^{n_{max}}(\epsilon) = \frac{1}{\pi\sqrt{1-\epsilon^2}}\left[1 + \sum_{m=1}^{n_{max}}\sum_{n=0}^{m} t_{mn}\hat{\mu}_i^{(n)} T_m(\epsilon)\right], \tag{20}$$

where n_{max} is the maximum number of moments used in the calculation. A detailed analysis on the density of states using the KPM can be found in Ref. 26.

From Eq. (3), the bond energy for atom i can be integrated as

$$U_i^{\text{bond}} = 20b_{i\infty}\int_{-1}^{\epsilon_F}(\epsilon - \gamma_{i0}/2)n_i(\epsilon)d\epsilon, \tag{21}$$

where $\gamma_{i0}=(a_{i0}-a_{i\infty})/b_{i\infty}$. By substituting Eq. (16) into Eq. (21) and using the recurrence relation in Eq. (14) for $\epsilon T_m(\epsilon)$, we have

$$U_i^{\text{bond}} = 10b_{i\infty}\sum_{m=0}\sigma_i^{(m)}\int_{-1}^{\epsilon_F}\frac{1}{\pi\sqrt{1-\epsilon^2}}[T_{m+1}(\epsilon) - \gamma_{i0}T_m(\epsilon) + T_{m-1}(\epsilon)]d\epsilon. \tag{22}$$

The reduced response function $\hat{\chi}_m(\epsilon_F)$ are written as

$$\hat{\chi}_m(\epsilon_F) = \int_{-1}^{\epsilon_F}\frac{1}{\pi\sqrt{1-\epsilon^2}}T_{m-1}(\epsilon)d\epsilon. \tag{23}$$

By using the trigonometric form of T_m (Ref. 25) for Eq. (23), we then get

$$\hat{\chi}_m(\phi_F) = \begin{cases} -\dfrac{\sin(\phi_F)}{\pi} & m=0 \\ 1-\dfrac{\phi_F}{\pi} & m=1 \\ -\dfrac{\sin(m-1)\phi_F}{\pi(m-1)} & m\geq 2, \end{cases} \tag{24}$$

where $\phi_F=\cos^{-1}(\varepsilon_F)$. This expression is different from that in the analytic BOP which has the form

$$\hat{\chi}_m(\epsilon_F) = \begin{cases} 0 & m=0 \\ 1-\dfrac{\phi_F}{\pi}+\dfrac{2}{\pi}\sin 2\phi_F & m=1 \\ \dfrac{1}{\pi}\left(\dfrac{\sin(m+1)\phi_F}{m+1}-\dfrac{\sin(m-1)\phi_F}{m-1}\right) & m\geq 2. \end{cases} \tag{25}$$

Eventually the analytic form of the bond energy will be

$$U_i^{\text{bond}} = 10b_{i\infty}\sum_{m=0}^{n_{max}}\sigma_i^{(m)}[\hat{\chi}_{m+2}(\phi_F) - \gamma_{i0}\hat{\chi}_{m+1}(\phi_F) + \hat{\chi}_m(\phi_F)]. \tag{26}$$

As can be seen in Table III of Ref. 10, γ_{i0} is a small quantity. With γ_{i0} simply taken as 0, inserting Eq. (24) into Eq. (26) will yield the smeared Fermi KPM bond energy.[5] Following Eq. (16), the total number of electrons per atom on-site i is given by

$$N_i = 10\int^{E_F} n_i(E)dE = 10\sum_{m=0}\sigma_i^{(m)}\hat{\chi}_{m+1}(\phi_F). \tag{27}$$

Equation (27) determines ϕ_F, and then Eq. (26) will be used to calculate the bond energy. The force F_k^{bond} can also be derived as

$$F_k^{\text{bond}} = -\nabla_k U^{\text{bond}(n_{max})} = -\sum_{i\alpha,j\beta}\tilde{\Theta}_{i\alpha,j\beta}^{(n_{max})}\nabla_k H_{j\beta,i\alpha} \tag{28}$$

with the bond order $\tilde{\Theta}_{i\alpha,j\beta}^{(n_{max})}$ as

$$\tilde{\Theta}_{i\alpha j\beta}^{(n_{max})} = 2\sum_{m=1}^{n_{max}}\sum_{n=0}^{m}[\hat{\chi}_{m+2}(\phi_F) + \hat{\chi}_m(\phi_F)]t_{mn}n\hat{\xi}_{i\alpha j\beta}^{(n-1)}, \tag{29}$$

where $\hat{h}=(\hat{H}-a_\infty)/(2b_\infty)$ and $\hat{\xi}_{i\alpha j\beta}$ is the dimensionless interference path.[10] Up to now, we have derived the KPM expressions from an *infinite* linear chain, while we know that the analytic BOP were derived staring from a *semi-infinite* linear chain. This derivation procedure has illustrated the close relation between the KPM and the BOP, although initially they were proposed from different backgrounds.[4,7] In addition, we also obtained the KPM bond-order expression in Eq. (29) which has not been shown before. The expressions involved in the KPM and the BOP are summarized in Table I.

Table I shows that the expressions between the KPM and the BOP are the same for $n_i^{n_{max}}(\epsilon)$, N_i, U_{bond}, $\tilde{\Theta}_{i\alpha j\beta}$, and F_k^{bond} provided that the value of $\hat{\chi}_m(\epsilon_F)$ and associated Chebyshev parts have been replaced.

Next the KPM will be applied to study the structural trend of the nonmagnetic transition-metal series. It can be seen from Table I that the KPM and BOP lead to different expressions of $\hat{\chi}_m(\epsilon_F)$, and this difference will be reflected in the quantity inside the brackets of Eq. (26). γ_{i0} is a small quantity,[10] and therefore γ_{i0} will be simply taken as 0 for the following analysis. Defining

$$\hat{\Gamma}_m = \hat{\chi}_m + \hat{\chi}_{m+2}, \tag{30}$$

its behavior varying through the band will be analyzed.

Figure 3 shows that there are $(m-2)$ nodes for $\hat{\Gamma}_m$ (excluding the starting and the end points) either from the KPM or from the BOP. If the moments from two structures are identical up to the $(m-1)$th moment, and the mth moment is different between the two structures, then $\sigma_i^{(m)}$ will start to be different as implied by Eq. (17). Consequently, the number of crossing points in terms of band filling will be determined by $\hat{\Gamma}_m$ as implied by Eq. (26). As a result, there will be at least $(m-2)$ nodes for this energy difference with respect to

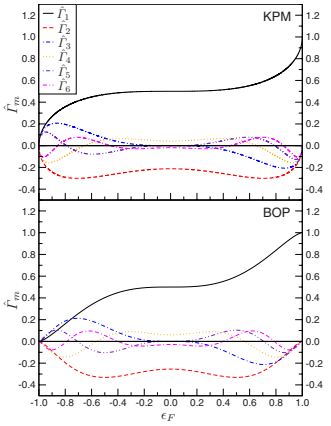

FIG. 3. (Color online) $\hat{\Gamma}_m$ as a function of ϵ_F from the KPM and the BOP.

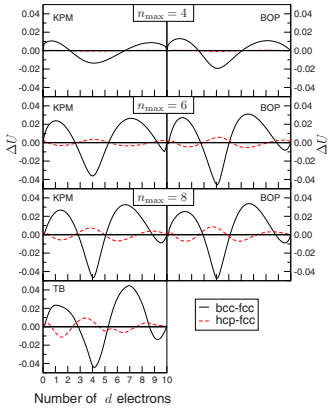

FIG. 4. (Color online) Normalized bond-energy difference $\Delta U = (U_{\text{bond}} - U_{\text{bond}}^{\text{fcc}})/|U_{\text{bond}}^{\text{fcc}}|$ as a function of number of d electrons from the KPM, BOP, and TB. The canonical values are used for the dd integrals (Ref. 27). The moments and the TB results are calculated from the BOPFOX code (Ref. 28). The KPM and the BOP results are obtained by programming in MATLAB.

the band filling. This is just the Ducastelle and Cyrot-Lackmann theorem.[18] Next the oscillatory behavior of the structural energy difference among bcc, fcc, and hcp will be studied with the use of both the KPM and the BOP.

The left-hand upper panel of Fig. 4 shows that the fourth moment from the KPM stabilizes the bcc for the half-full band. This is similar to the results from the analytic BOP (Ref. 10), which is plotted at its right-hand panel. Figure 4 also shows that the six-moment contribution is needed to differentiate the fcc and hcp stabilities. The KPM is able to predict the observed structural trend from hcp→bcc→hcp→fcc across the nonmagnetic transition-metal series (except $N=9$, where the *sp-d* hybridization contribution becomes significant[2]). It can also be seen that the KPM results are nearly the same as the BOP results and both of them converge quickly at low order to the TB results as the number of moments increases.

In summary, we have analyzed the two moment-based potential construction methods: the KPM and the BOP. The KPM was derived in a similar procedure where the analytic BOP has been derived. It shows that the *infinite* linear chain can lead to the KPM by using the first-kind Chebyshev polynomials, while the *semi-infinite* linear chain leads to the analytic BOP by using second-kind Chebyshev polynomials. We found that the mathematical formulas for the average density of states, bond energy, bond order, and the force between the KPM and the BOP are the same if the corresponding Chebyshev parts are replaced. Historically the potential construction based on $T_m(\epsilon)$ is called KPM while that based on $P_m(\epsilon)$ is called BOP. But we can see that the KPM gets a bond-order expression, so it can be called a bond-order potential; on the other hand, the BOP is a kernel polynomial method. So their names may not tell the difference. We analyzed that the KPM, like the BOP, is also able to explain the structural trend of the nonmagnetic transition-metal series.

The author gratefully thanks D. G. Pettifor, R. Drautz, T. Hammerschmidt, and B. Seiser for providing the BOPFOX package.

*tqin77@googlemail.com

[1] A. P. Sutton, *Electronic Structure of Materials* (Oxford University Press, Oxford, 1993).
[2] D. G. Pettifor, *Bonding and Structure of Molecules and Solids* (Oxford University Press, Oxford, 1995).
[3] M. Finnis, *Interatomic Forces in Condensed Matter* (Oxford University Press, Oxford, 2003).
[4] R. N. Silver and H. Röder, Int. J. Mod. Phys. C **5**, 735 (1994).
[5] A. F. Voter *et al.*, Phys. Rev. B **53**, 12733 (1996).
[6] A. Weisse *et al.*, Rev. Mod. Phys. **78**, 275 (2006).
[7] R. Haydock, Solid State Phys. **35**, 216 (1980).
[8] D. G. Pettifor, Phys. Rev. Lett. **63**, 2480 (1989).
[9] A. P. Horsfield *et al.*, Phys. Rev. B **53**, 12694 (1996).
[10] R. Drautz and D. G. Pettifor, Phys. Rev. B **74**, 174117 (2006).
[11] S. Goedecker, Rev. Mod. Phys. **71**, 1085 (1999).
[12] G. Galli and M. Parrinello, Phys. Rev. Lett. **69**, 3547 (1992).
[13] F. Mauri *et al.*, Phys. Rev. B **47**, 9973 (1993).
[14] X. P. Li *et al.*, Phys. Rev. B **47**, 10891 (1993).
[15] M. S. Daw, Phys. Rev. B **47**, 10895 (1993).
[16] M. Mrovec *et al.*, Phys. Rev. B **75**, 104119 (2007).
[17] M. Cini, *Topics and Methods in Condensed Matter Theory: From Basic Quantum Mechanics to the Frontiers of Research* (Springer, Berlin, 2007).
[18] F. Ducastelle and F. Cyrot-Lackmann, J. Phys. Chem. Solids **31**, 1295 (1970).
[19] A. P. Sutton *et al.*, J. Phys. C **21**, 35 (1988).
[20] H. J. Gotsis *et al.*, Phys. Rev. B **65**, 134101 (2002).
[21] H. Amara *et al.*, Phys. Rev. B **79**, 014109 (2009).
[22] C. Lanczos, J. Res. Natl. Bur. Stand. **50**, 255 (1950).
[23] R. Haydock *et al.*, J. Phys. C **5**, 2845 (1972).
[24] R. Haydock *et al.*, J. Phys. C **8**, 2591 (1975).
[25] M. Abramowitz and I. A. Stegun, *Handbook of Mathematical Functions: With Formulas, Graphs, and Mathematical Tables*, 9th ed. (Dover, New York, 1973).
[26] R. N. Silver *et al.*, J. Comput. Phys. **124**, 115 (1996).
[27] O. K. Andersen *et al.*, Phys. Rev. B **17**, 1209 (1978).
[28] T. Hammerschmidt, B. Seiser, D. G. Pettifor, and R. Drautz, BOPFOX code, 2008.